REVISITING ENHANCED AIS DETECTION RANGE UNDER DUCTING

Irina Sirkova

Laser Radars Lab, Institute of electronics, Bulgarian Academy of Sciences,
Tzarigradsko chaussee 72, 1784 Sofia, Bulgaria
irina@ie.bas.bg

Abstract

This report studies the propagation of Automatic Identification System frequencies under various tropospheric ducting and sea surface conditions with the parabolic wave equation method. The aim is to examine the influence of sea surface roughness on the possibility to enlarge the AIS detection range under ducting.

1. INTRODUCTION

Initially designed as a ship reporting system for collision avoidance, the AIS (Automatic Identification System) nowadays has enlarged applications beyond the situational awareness and security. The AIS has become part of the VHF Data Exchange System concept [1] which increases the requirements to the AIS performance and reliability. At the same time, the growing importance of the AIS traffic poses the need to monitor shipping at distances greater than can be achieved via the conventional propagation mechanisms like line-of-sight (LoS) and diffraction. Thus the long range detection capability becomes a key AIS characteristic. Among the factors that can influence the long range detection of AIS messages the ducting anomalous propagation mechanism, often present over the sea, is identified as a major candidate [2]. This clear-air propaga-tion mechanism is due to deviation in tropospheric refractivity *N* (N=(n-1)10^6) from the standard conditions caused by temperature and water vapour changes. The spatial change of *n* is larger with height than with range and generally the horizontal variations of *n* can be neglected [3]. The appearance of negative vertical gradient of the modified refractivity *M* (M=N+(z/a_e)10^6, with *z* the height above the sea surface and a_e - the Earth's radius, indicates the presence of tropospheric duct [3]. For practical purposes the average behaviour of the modified refractivity *M*(*z*) is often approximated with piecewise-linear profile. On Fig. 1 are schematically presented the *M*(*z*) profiles for the four duct types with essential parameters indicated.

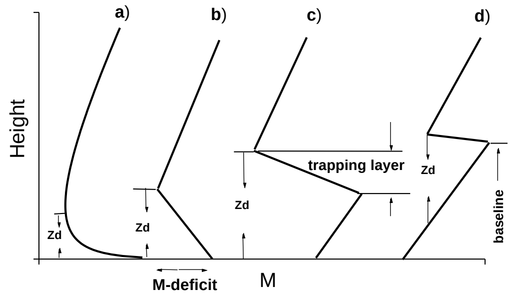

Figure 1. a) evaporation, b) surface, c) surface-based, d) elevated duct, zd – duct thickness

The complicated maritime conditions require sophisticated propagation methods. The paraxial approximation to the wave equation, known as the parabolic equation (PE), allows correct accounting simultaneously for the strong refraction under ducting, dif-fraction around the Earth's curvature, reflection and scattering from the rough sea surface, and antenna pattern [4, 5]. This report studies the propagation of AIS frequencies under various tropospheric ducting and sea surface conditions with the PE method. The aim is to examine the influence of sea surface roughness on the possibility to enlarge the AIS detection range under ducting.

2. METHOD DESCRIPTION

In this study 2D narrow-angle forward-scatter scalar PE is used as implemented in "Advanced propagation model (APM) Computer software configuration item (CSCI) documents", Space and Naval Warfare Systems Center Tech. Doc. 3145, which allows finding a full-wave solution to the AIS signal propagation problem in terms of path loss, *PL* (*PL* in dB):

$$PL = 20\log\left(\frac{4\pi r}{\lambda}\right) - PF\ , \qquad (1)$$

here λ is the free-space wavelength, r is the distance between the corresponding points and PF is the propagation factor (in dB) defined as the square of the ratio of the electric field amplitude E received at a given point under specific conditions to the amplitude of the electric field E_0 received at the same point under free-space conditions where E participates with its polarization component which coincides with the polarization of E_0 [3]. In this study, the initial field is provided by an omni directional antenna. Equation (2) gives the expression of the PF in terms of the reduced PE field, $U(x,z)$, which comes from the APM routines:

$$PF = 20\log|U(x,z)| + 10\log(r) + 10\log(\lambda)\ . \qquad (2)$$

Two international channels in the VHF maritime mobile band centered at 161.975 MHz and 162.025 MHz are allocated to the AIS. Later in the calculations the F=161.975 MHz is used. The examples of duct parameters have been taken from among the typical ones for the Bulgarian Black sea shore [6]. In order to preliminary assess the trapping of the AIS frequencies, well known formula for maximum wave length, λ_{max}, trapped in a duct is used [7]:

$$\lambda_{max} = \frac{2}{3} C z_d (\Delta M)^{1/2}\ , \qquad (3)$$

where z_d is the duct thickness, ΔM is the M-deficit, see Fig. 1, and C=3.77x10^{-3} for surface and surface-based ducts. In this report these two types of ducts have been studied: the evaporation duct, even though the most widespread over the sea, is not able to trap the AIS frequencies with its maximal height of 40 m, whereas the elevated ducts have been considered to have weak influence due to there relatively great height above the sea surface. Also, surface and surface-based ducts are less sensitive to frequency than evaporation ducts and can extend over the ocean for several hundreds of kilometers and last for multiple days.

A trans-horizon path supposes reflections from the sea surface, therefore the sea surface roughness should be accounted for. Here this is done in the framework of the "effective" reflection coefficient, R_{eff}, concept in which the Fresnel reflection coefficient, R_F, is multiplied by a roughness reduction factor R_{rf} [4]:

$$R_{eff} = R_{rf} R_F\ , \qquad (4)$$

$$\begin{aligned} R_{rf} = R_{\mathrm{M-B}} = \exp\left[-2k^2\sigma_h^2 \sin^2(\alpha)\right] \mathrm{x} \\ \mathrm{I}_0\left[2k^2\sigma_h^2 \sin^2(\alpha)\right]. \end{aligned} \qquad (5)$$

In (5) the Miller-Brown roughness reduction coefficient, $R_{\mathrm{M-B}}$, is used [8] where σ_h is the standard deviation of the sea surface height h, I_0 is the modified Bessel function of the first kind of order zero, k is the free-space wave number and α is the local grazing angle measured with respect to the mean plane of the sea surface. The $R_{\mathrm{M-B}}$ assumes the sea wave amplitude is Gaussian distributed with zero mean, i.e. in (5) $\sigma_h = h_{rms}$ where h_{rms} is the root mean square deviation of the surface height. Note that the $R_{\mathrm{M-B}}$ refers to the forward coherent reflected field (i.e. the diffuse scattered field is neglected as well as the small perturbations of the sea surface) and does not account for the shadowing and multiple scattering. The only parameter related to sea surface roughness in $R_{\mathrm{M-B}}$ is the h_{rms} which can be expressed entirely in terms of the wind speed. In (5) the quantity $2kh_{rms}\sin(\alpha)$ is the Rayleigh roughness parameter for the surface, [4], that is often used as a criterion for the degree of roughness. It is to note that when the grazing angles are very small (both ducting propagation and ship-to-ship propagation suppose small grazing angles) $R_{\mathrm{M-B}}$ tends to 1 and thus the influence of the roughness is reduced. Nevertheless, the wavelength of AIS frequencies is about 1.85 m, i.e. it is of the same order as sea height variations in high sea states; hence, a roughness reduction factor is to be introduced to account for the reduction of the Fresnel reflection coefficient from flat surface.

There is a variety of formulae relating h_{rms} to the wind speed and sea state [9, 10] depending on the sea wave spectrum used for their obtaining. In this report the relation corresponding to sea wave spectra of Pierson-Moskowitz type is applied [10]:

$$h_{rms} = 0.0051 U_{10}^2\ , \qquad (6)$$

where U_{10} is the wind speed in m/s at h=10 m. The dielectric characteristics of the sea surface are calculated as functions of frequency following "Propagation in Non-Ionized Media", CCIR 1986, vol.5.

3. RESULTS AND DISCUSSION

The first example of ducted propagation refers to a surface duct with bilinear profile (see Fig. 1 (b)) and parameters z_d=100 m, ΔM=45 M-units, antenna height h_a=10 m, F=161.975 MHz, horizontal polarization (HOR) and smooth sea surface. It is to note that, following relation (3), this duct requires

λ_{max}<1.68 m; this means that AIS frequencies (λ around 1.85 m) will not be (completely) trapped. However, the transition from ducting to non-ducting conditions (and vice versa) for frequencies with λ around λ_{max} is gradual and those frequencies will have significantly extended propaga-tion/ detection range in comparison to the standard troposphere case, see Fig. 2 and Fig. 3. On Fig. 2 is shown path loss versus range and height. Figure 3 provides the *PL* for two vertical cuts at fixed range *FixR*=20 km and *FixR*=25 km (red and black line); for comparison are given the respective cuts for standard troposphere (StanTrop) - green and blue line. Even for these relatively short distances, 20 km and 25 km, the *PL* decrease under ducting is clearly seen, especially for the most important first 50 meters above the sea surface. With some certainty it can be expected that under similar conditions the AIS detection range will be increased.

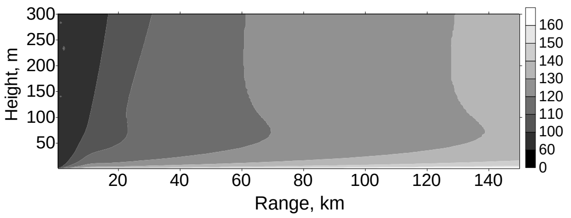

Figure 2. *PL* for surface duct

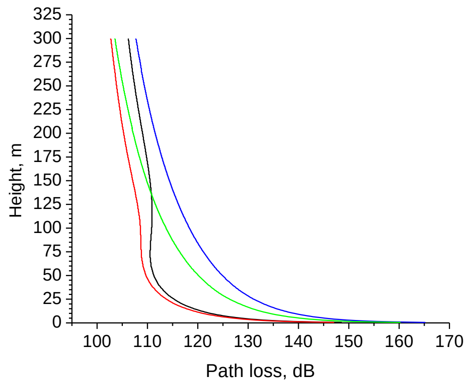

Figure 3. PL for FixR=20 km (red – surface duct, green - StanTrop) and FixR=25 km (black – surface duct, blue - StanTrop)

The next four figures, Fig.4 - Fig.7, refer to a surface-based duct modelled with tri-linear profile (see Fig. 1 (c)) with parameters as follows: trapping layer base height 113 m, z_d=268 m, ΔM=23 M-units, the slopes of the profile below and above the trapping layer correspond to the standard troposphere. The AIS frequencies are trapped by this duct. The *PL* for h_a=20 m and HOR is shown on Fig. 4 for standard troposphere, smooth and rough sea (U_{10}=9 m/s). On Fig. 5 are shown *PL* curves for fixed height FixH=h_a=20 m for the tri-linear duct and smooth sea: black curve refers to HOR, red for VER (vertical polarization); for comparison the respective curves for StanTrop are also given (in blue and green). Clearly seen is the difference between the two polarizations. Note that close to the two *PL* peaks the *PL* under ducting exceeds that of standard troposphere. After the second peak ducting decreases significantly the *PL* but it exists a "skip zone" between 20th and 60th km, see Fig. 4 (b).

On Fig. 6 are shown *PL* curves for fixed range *FixR*=35 km (close to the first *PL* peak, see Fig. 5) for the same tri-linear duct as on Figs. 4 and 5, and HOR: the red curve refers to smooth sea, the StanTrop *PL* is given in blue, the black curve shows the influence of sea surface roughness introduced through formulas (4)-(6) for U_{10}=9 m/s. Figure 7 presents the *PL* for the same conditions as on Fig. 6 but only the area of interest below the first 50 meters above the sea is given: red - smooth sea; black - rough sea, U_{10}=9 m/s; blue - rough sea, U_{10}=15 m/s. As expected, the influence of ducting prevails over that of sea roughness which is negligible except in the area close to the *PL* peak. A possible reason is change of the grazing angles to the sea in the "skip zone" so that the influence of the R_{rf}=$R_{M\text{-}B}$ is increased. The increased roughness, U_{10}=15 m/s, "blurs" the *PL* pattern, see also Fig. 4 (c). The presence of "skip zones" indicates that ducting may not always be advantageous for the detection range and this may by aggravated by the sea roughness.

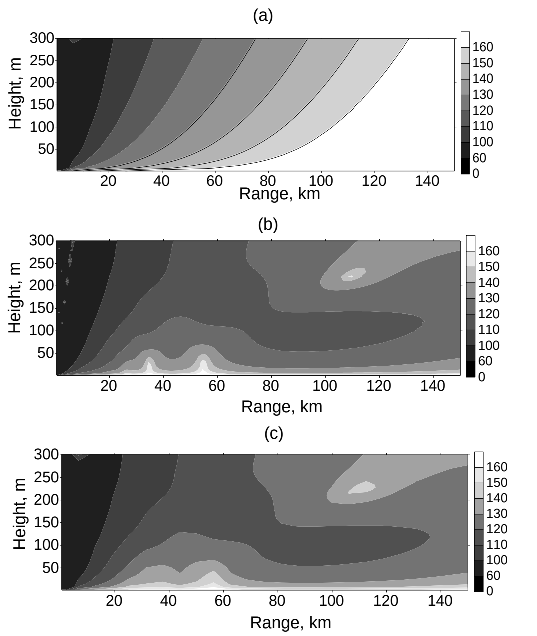

Figure 4. *PL* for h_a=20 m: (a) StanTrop, (b) tri-linear duct, smooth sea, (c) tri-linear duct, rough sea

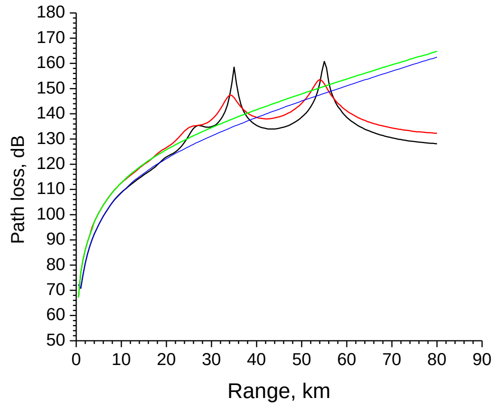

Figure 5. *PL* for FixH=h_a=20 m, tri-linear duct, smooth sea: black – HOR, red – VER, blue & green – HOR & VER for StanTrop

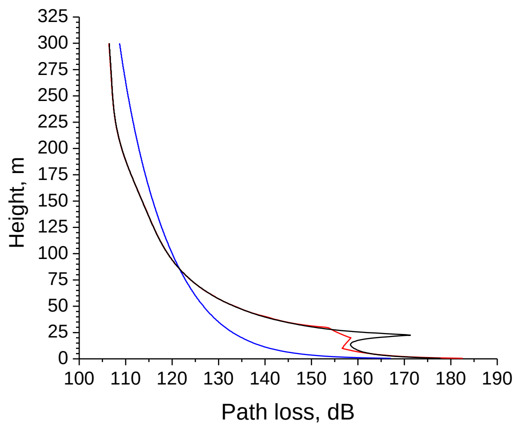

Figure 6. PL for FixR = 35 km, HOR, tri-linear duct: red - smooth sea, black – rough sea, blue – StanTrop

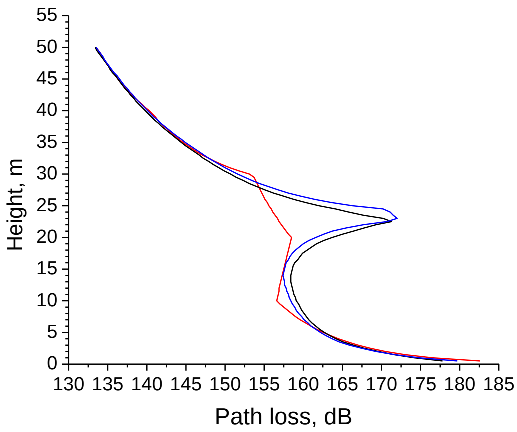

Figure 7. PL for FixR=35 km, HOR, tri-linear duct: red - smooth sea, black – rough sea, U10=9 m/s, blue - rough sea U10=15 m/s

4. CONCLUSION

The results indicate that to be reliable and of practical use the extension of the detection range through ducting requires:

– a good preliminary assessment of the duct types and parameters;

– accounting for sea roughness for sea state 4 and higher (according to the scale relating wind speed to sea state [10]); even though the roughness has rather weak influence, it may increase the *PL* in the "skip zones";

– additional investigations that account for the rocking of the ship, influence of breaking waves, etc.

5. ACKNOWLEDGMENTS

This work was supported by the Ministry of Education and Science of Bulgaria (support for ACTRIS BG, part of the Bulgarian National Roadmap for Research Infrastructure).

References

[1] F. Lázaro, R. Raulefs, W. Wang et al. "VHF Data Exchange System (VDES): an enabling technology for maritime communications", CEAS Space J, Vol. 11, 2019, 55–63.

[2] ITU-R M.2123 "Long range detection of automatic identification system (AIS) messages under various tropospheric propagation conditions", 2007.

[3] D.E. Kerr, (Ed.) Propagation of Short Radio Waves, Peter Peregrinus, London, UK, 1987.

[4] M. Levy, Parabolic Equation Methods for Electromagnetic Wave Propagation, IEE electromagnetic waves series 45, UK, 2000.

[5] I. Sirkova, "Brief Review on PE Method Application to Propagation Channel Modeling in Sea Environment", CEJE, Vol. 2, No. 1, 2012, 19-38.

[6] I. Sirkova, "Duct occurrence and characteristics for Bulgarian Black sea shore derived from ECMWF data", J Atmos Sol-Terr PHy, Vol. 135, 2015, 107-117.

[7] J. D. Turton, D. A. Bennetts, and S.F.G. Farmer, "An introduction to radio ducting," Meterorolog. Mag., Vol. 117, 1988, 245-254.

[8] A. R. Miller, R. M. Brown, and E. Vegh, "New Derivation for the Rough Surface Reflection Coefficient and for the Distribution of Sea-Wave Elevations", IEE Proc.-H, Vol. 131, 1984, 114–116.

[9] T. P. Leonard, I. Antipov, and K.D. Ward, "A comparison of radar sea clutter models", Conf. Radar 2002, 15-17 Oct 2002, Edinburgh, UK, 429-433.

[10] L. B. Wetzel, "Sea clutter", Naval Res. Lab. Report 9244, Washington, USA, 1990, 41 p.